Force Commutated Three Level Boost Type Rectifier

Yifan Zhao, Yue Li, and Thomas A. Lipo, *Fellow, IEEE*

Abstract— **A new force commutated three level boost type rectifier is proposed in this paper. The rectifier has the characteristics of drawing nearly sinusoidal current from utility with unity fundamental power factor. High reliability is possible due to its shoot-through free structure. A doubled dc bus voltage compared to a normal two-level rectifier is also possible because of the neutral point clamping. The operating principle, steady state analysis, input current and neutral point voltage control schemes, as well as detailed experimental results are presented in this paper.**

I. Introduction

THE thyristor bridge rectifier is the most widely used interface between utility and power electronics systems or any other system where dc power supplies are required. Although the thyristor bridge rectifier is very simple in structure and robust in operation, it has the disadvantages of drawing a large amount of harmonic current from utility and causing utility pollution. As more and more power electronics systems are being used in industry, it can be expected that the utility pollution problem will become increasingly intolerable. Therefore, standards such as IEEE 519 have been proposed that may eventually lead to limiting the direct use of the thyristor bridge rectifier as the interface. At the same time, much effort has been made with the low harmonic current injection to utility and controllable input power factor as major goals.

In this paper, a new interface topology called a force commutated three level rectifier is presented. The proposed rectifier is capable of drawing nearly sinusoidal current from the utility with either unity fundamental power factor, or the ability of absorbing or delivering a certain amount of controllable reactive power to the utility. As the basic topology of this circuit is a diode rectifier, it has the limitation of the unidirectional active power follow. The paper focuses its discussions on the operating principle, operating range, and input current control scheme of this new topology. Experimental results are presented. Voltage balancing among the series connected dc bus capacitors, a common problem with multi-level converters is also treated in this paper.

II. Operating Principle and Steady State Analysis

The proposed three level boost type rectifier is shown in Fig. 1. It consists of three switching arms with each one has four diodes and two active switches. The operating principle is illustrated as follows. For switching arm 1, the rectifier input terminal voltage v_{un} is clamped to the neutral point of the dc bus when switches S_{11}, and S_{12} are "on." When S_{11}, S_{12} are "off," v_{un} can be either $+\frac{V_{dc}}{2}$ or $-\frac{V_{dc}}{2}$ according to the polarity of the current in phase A. Therefore, switching arm 1 has three switching states, namely "1," "0," and "-1," which indicate whether the rectifier input terminal U is clamped to positive dc bus, neutral point, and negative dc bus respectively. The same analysis also applies to the rest of the switching arms. As the rectifier has three switching arms, the total number of switching modes of the rectifier is $3^3 = 27$. The number of distinguishable voltage vectors produced by the 27 switching modes is 19. The switching modes and the voltage vectors for this circuit are shown in Fig. 2.

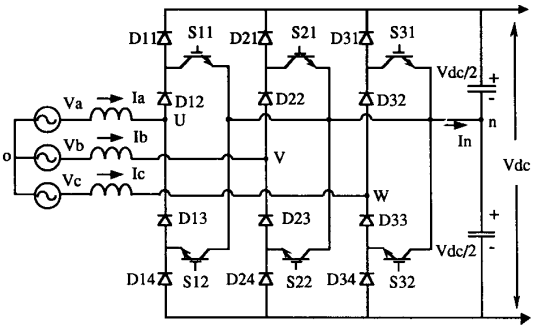

Fig. 1. Proposed circuit configuration.

It can be noted that because of the existence of the dc bus neutral point, the maximum voltage stress on each device is $\frac{V_{dc}}{2}$. This feature enables the rectifier output voltage to be double the dc bus voltage compared with a conventional PWM type rectifier with same switching device voltage rating. Another significant advantage of the proposed topology is that the shoot-though current is blocked by the diodes connected to the dc buses even when both the active switches in a switching arm are "on." This provides for high reliability of the rectifier.

Referring to the utility-rectifier equivalent circuit shown in Fig. 3, from fundamental circuit theory it can be determined that for the input current to be sinusoidal the rectifier input terminal voltage V_{u0}, V_{v0}, and V_{w0} must be sinusoidal as well. Although it is impossible, one could conceive of synthesizing these voltages using the voltage vectors in Fig. 2 in a manner that the rectifier input terminal voltage has a desired fundamental component with only high frequency harmonics. By this procedure, the input harmonic current will be small due to the low pass characteristic of the input inductors. In addition to concerns regarding the input current harmonic content, it is also required that the amplitude and the phase angle of

Paper IPCSD 94–50, approved by the Industrial Power Converter Committee of the IEEE Industry Applications Society for presentation at the 1993 Industry Applications Society Annual Meeting, Toronto, Ontario, Canada, October 3–8. Manuscript released for publication June 23, 1994.

The authors are with Department of Electric and Computer Engineering, University of Wisconsin, Madison, WI 53706 USA.

IEEE Log Number 9406607.

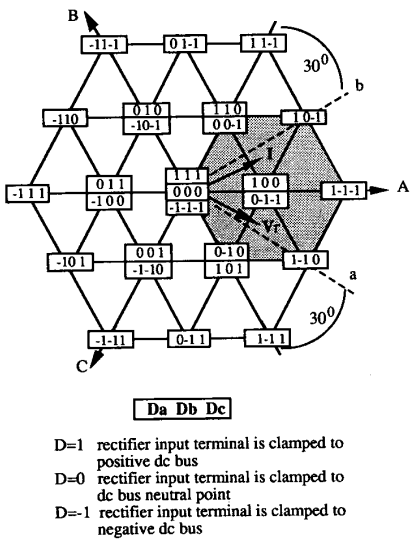

Fig. 2. Switching modes and limitations on voltage vector realization.

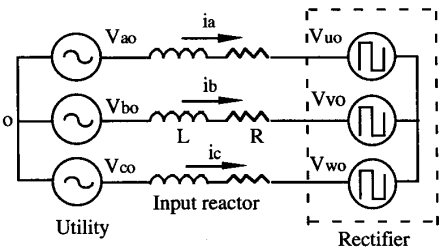

Fig. 3. Utility rectifier equivalent circuit.

the rectifier input terminal voltage should be controllable in order to control the amplitude and the phase angle of the input current. However, it should be pointed out that for the proposed circuit configuration only a portion of the 19 voltage vectors are realizable at any instant of time. Consider the case in Fig. 2, for the given current vector position, $i_a > 0$, $i_b < 0$ and, $i_c < 0$. Here, switching state "-1" is not realizable in leg 1 because the positive current of phase A cannot flow through diodes D_{13} and D_{14}. For the same reason, state "$+1$" is not possible in both leg 2 and leg 3 for that input current vector position. By eliminating all the switching modes containing the unrealizable states, a hexagon shaped shaded area can be determined which contains the realizable switching modes and voltage vectors. This area moves as the current vector rotates in the vector space. Because of the restricted switching mode realization, it is necessary to investigate its impact on the input current control.

Again referring to Fig. 2, it can be noted that as long as the current vector $\mathbf{I}$ stays in the region bounded by the dashed lines a and b, the shaded hexagon area will stay at the position shown. Also note that the voltage vector $\mathbf{V}_r$ corresponding to the desired rectifier input terminal voltage vector must remain in this area due to the limitations discussed before. The two worst cases occur when the current vector $\mathbf{I}$ is at the position of

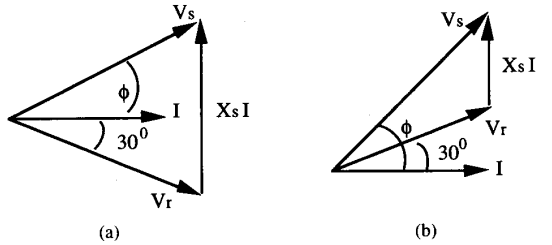

Fig. 4. Phasor diagrams for critical operation. a) 30° leading, $\mathbf{I}$ versus $\mathbf{V}_r$; b) 30° lagging, $\mathbf{I}$ versus $\mathbf{V}_r$.

line a and the lead angle of $\mathbf{I}$ with respect to $\mathbf{V}_r$ is greater than 30°, and when $\mathbf{I}$ is at the position of line b with a 30° lagging condition. In both cases the vector $\mathbf{V}_r$ is required outside the hexagon and thus is unrealizable. The phasor diagrams of the two critical cases are drawn in Fig. 4 (where the resistance R of the input reactor is neglected).

From the phasor diagram in Fig. 4(a) one can derive the following equation for the input current.

$$I_{\max}(\text{p.u.}) = 1.155\sin(\phi + 30°) \tag{2.1}$$

where ϕ is the input current displacement angle.

The current $I_{\max}$ is the maximum current that the rectifier can draw from utility without low frequency harmonic distortion. It is a p.u. value with $V_b = V_s$, the rms phase voltage of utility, and $I_b = \frac{V_b}{X_s}$, the rectifier input terminal short circuit current, where $X_s = \omega L$.

Another equation derived from Fig. 4(b) is:

$$I_{\max}(\text{p.u.}) = 1.155\sin(\phi - 30°). \tag{2.2}$$

The current $I_{\min}$ is the minimum current that the rectifier must draw from utility to avoid low frequency harmonic distortion.

Equations (2.1) and (2.2) define the limits of the operation region of the proposed rectifier as shown in Fig. 5(a). The maximum input power and reactive power can be easily derived from (2.1) and are shown in Fig. 5(b) with:

$$P_{\max}(\text{p.u.}) = 1.155\sin(\phi + 30°)\cos(\phi) \tag{2.3}$$

$$Q_{\max}(\text{p.u.}) = 1.155\sin(\phi + 30°)\sin(\phi). \tag{2.4}$$

III. Input Current and DC Bus Neutral Point Voltage Control

The steady state analysis in the previous section is based on the assumption that the voltage across the dc bus capacitors is balanced. In reality the neutral point voltage is inclined to drift due to an arbitrary unbalanced operation due to slight imperfections in circuit. Therefore, explicit control over the neutral point voltage must be exercised together with input current control to guarantee correct operation of the rectifier.

A. Neutral Point Voltage Control

Neutral point voltage control is achieved by using the voltage vectors in the center of each shaded hexagon. In Fig. 2, this vector is produced by switching modes 1, 0, 0 and 0, -1, -1. Because each of these vectors corresponds to two switching modes, and the two switching modes produce

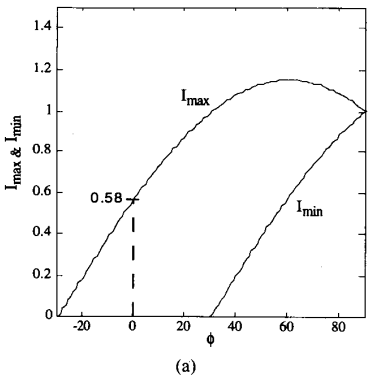

(a)

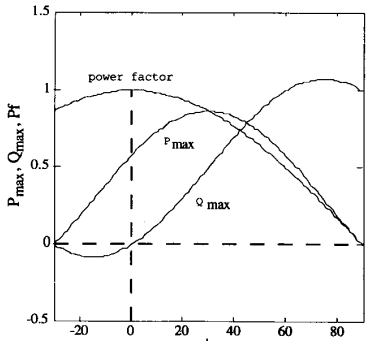

(b)

Fig. 5. Steady state analysis results. (a) Operating region for input current. (b) Maximum power and reactive power, power factor.

different polarities of neutral current I_n, two degrees of freedom exist to control the input current and neutral point voltage simultaneously. In particular if the voltage vector at the center of the shaded area in Fig. 2 is demanded by the current controller, one can choose either switching mode 1, 0, 0 or switching mode 0, -1, -1 to produce this voltage vector. When mode 1, 0, 0 is chosen, rectifier input terminals V and W are clamped to the neutral point. Because input current I_b and I_c are negative, neutral current I_n is forced to flow out of the neutral point. As a result, the neutral point voltage will drift towards the negative dc bus. On the other hand if switching mode 0, -1, -1 is chosen, the neutral point voltage will drift toward the positive dc bus since the neutral current now becomes positive.

B. Current Control Scheme

Theoretically, almost all the control schemes developed for inverter current control can be employed for the purpose of current control of this converter. Among these schemes, the hysteresis controller is the choice for the method with greatest simplicity of implementation. When a hysteresis controller is used, the voltage vectors are randomly chosen from a hexagon which contains seven possibilities. Therefore, the chance of the voltage vector capable of controlling neutral point voltage being selected is only one in seven. This degree of control does not appear to be sufficient for the purpose of neutral point voltage control. Based on experience with the circuit, it appears that the best current control scheme for the proposed rectifier should be the one with not only fast response to the input current error, but also a strong ability to handle the neutral point voltage drifting problem. For this purpose, a special current control scheme was adopted with some modifications. The scheme utilizes current deviation vector in determining switching modes and offers great flexibility in compromising between input current and neutral point voltage control.

The principle of the current control scheme is illustrated as follows.

The voltage equation for the power supply-rectifier equivalent circuit shown in Fig. 3 can be expressed as:

$$\mathbf{V}_s = L\frac{d\mathbf{I}}{dt} + R\mathbf{I} + \mathbf{V}_r(k) \tag{3.1}$$

where

$$\mathbf{V}_s = \begin{bmatrix} v_a \\ v_b \\ v_c \end{bmatrix}, \text{ power supply phase voltage vector,}$$

$$\mathbf{I}_s = \begin{bmatrix} i_a \\ i_b \\ i_c \end{bmatrix}, \text{ rectifier input current vector,}$$

$$\mathbf{V}_r(k) = \begin{bmatrix} v_{u0} \\ v_{v0} \\ v_{w0} \end{bmatrix}, \text{ instantaneous input terminal voltage,}$$

$$k = 0, \ldots, 18.$$

Defining $\Delta\mathbf{I} = \mathbf{I}^* - \mathbf{I}$ and substituting into (3.1) yields:

$$L\frac{d(\Delta\mathbf{I})}{dt} = \mathbf{V}_r(k) - \mathbf{E} \tag{3.2}$$

where

$$\Delta\mathbf{I} = \begin{bmatrix} i_a^* - i_a \\ i_b^* - i_b \\ i_c^* - i_c \end{bmatrix}, \text{ current deviation vector,}$$

$$\mathbf{I}^* = \begin{bmatrix} i_a^* \\ i_b^* \\ i_c^* \end{bmatrix}, \text{ input current reference vector, and}$$

$$\mathbf{E} = \mathbf{V}_s - \left(L\frac{d\mathbf{I}^*}{dt} + R\mathbf{I}^*\right) = \begin{bmatrix} e_a \\ e_b \\ e_c \end{bmatrix} \tag{3.3}$$

Let $v_a = V_m \sin(\omega t)$, $i_a^* = I_m^* \sin(\omega t - \phi)$, and substitute these expressions into (3.3). The following equations can be determined:

$$\mathbf{E} = \begin{bmatrix} E_m \sin(\omega t - \theta) \\ E_m \sin(\omega t - \theta - 120^\circ) \\ E_m \sin(\omega t - \theta + 120^\circ) \end{bmatrix} \tag{3.4}$$

where

$$E_m = \sqrt{(V_m)^2 + (\omega L I_m^*)^2 - 2V_m \omega L I_m^* \sin(\phi)}$$

$$\theta = \cos^{-1}\left(\frac{V_m - \omega L I_m^* \sin(\phi)}{E_m}\right).$$

The resistance of the input reactor is neglected in (3.4).

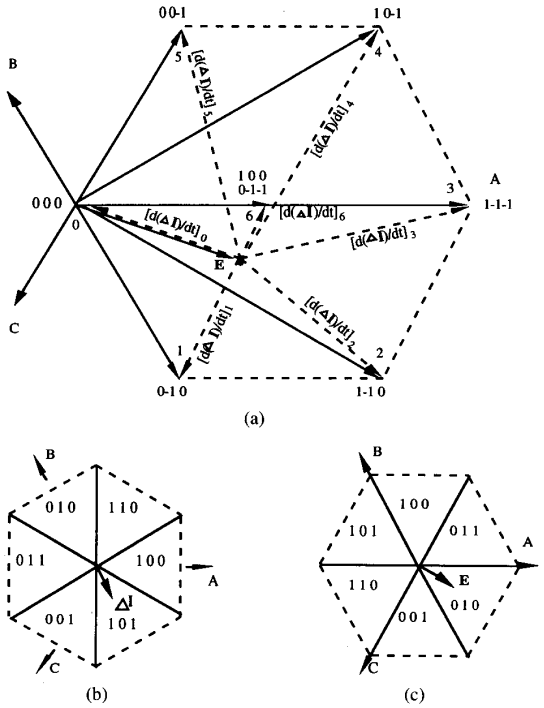

Fig. 6. Switching mode selection. (a) Realizable switching modes for a particular position of input current vector and the derivatives of current deviation vector. (b) Regions for input current vector and deviation current vector. (c) Regions for vector **E**.

Equation (3.4) shows that **E** can be easily determined by the current command I^*, supply voltage $\mathbf{V}_s$, and the input reactor inductance L. Returning to (3.2) one can find that $\mathbf{V}_r(k)$ can be selected according to the position of vector **E** and position of the current deviation vector $\Delta\mathbf{I}$ such that the direction of $\frac{d(\Delta\mathbf{I})}{dt}$ is always trying to decrease the deviations of the real current from the current command.

C. Selection of Switching Modes

For the proposed rectifier, as previously mentioned, a compromise must be reached between the control of the input current and the control of neutral point voltage. Another characteristic of the proposed rectifier is that for any given position of the input current vector, the realizable switching modes are confined in a small hexagon around that vector. These two factors determine the rules of the switching mode selection.

Assume that the vectors **I**, **E** and the corresponding realizable switching modes are at the position shown in Fig. 6(a). The hexagon in Fig. 6(a) is the same as the shaded area in Fig. 2. The $\frac{d(\Delta\mathbf{I})}{dt}$ vectors corresponding to $\mathbf{V}_r(k)$ (where $k = 0, \ldots, 6$) are also shown in Fig. 6(a). Where in Fig. 6(a), the switching modes that can be used to control the neutral point voltage are 0, -1, -1 and 1, 0, 0, which are at the center of the hexagon. Fig. 6(b) shows the regions to which the current deviation vector $\Delta\mathbf{I}$ may belong.

From Fig. 6(a) and (b), if only input current control is considered, one can summarize the relations between the position of $\Delta\mathbf{I}$ and the switching modes as in Table I. Here the rule for the selection of switching modes is to select the one that will produce the vector $\frac{d(\Delta\mathbf{I})}{dt}$ in the direction most opposite to $\Delta\mathbf{I}$. As an example, for the $\Delta\mathbf{I}$ position in Fig. 6(b), the $\frac{d(\Delta\mathbf{I})}{dt}$ vector produced by switching mode $0, 0, -1$ (vector $\mathbf{V}_r(5)$) should be selected.

TABLE I
SWITCHING MODE SELECTION (CONSIDER ONLY INPUT CURRENT CONTROL)

Position of $\Delta\mathbf{I}$	101	100	110	010	011	001
Switching modes	00-1	000	0-10	1-10	1-1-1	100 0-1-1 10-1

TABLE II
SWITCHING MODE SELECTION (CONSIDER BOTH INPUT CURRENT CONTROL AND NEUTRAL POINT VOLTAGE CONTROL)

Position of $\Delta\mathbf{I}$	101	100	110	010	011	001
Switching modes	100 0-1-1	000	0-10	1-10	100 0-1-1	100 0-1-1

Table II also shows the relations between the positions of $\Delta\mathbf{I}$ and the switching modes but with the neutral point voltage control being taken into consideration. Here the rule becomes to choose vector $\mathbf{V}_r(6)$ (switching modes 1, 0, 0 or 0, -1, -1) as many times as possible as long as the dot products of $\Delta\mathbf{I}$ and $[\frac{d(\Delta\mathbf{I})}{dt}]_6$ are not positive, i.e., the length of $\Delta\mathbf{I}$ does not increase.

Comparing the two tables it is possible to determine that the chances of voltage vector 6 being selected in Table II is three times larger than that in Table I. Therefore the switching mode selection method in Table II offers a strong control action over the neutral point voltage. The trade-off is that this method has a somewhat slower response to minimize the current error.

D. Implementation of the Switching Modes Selection Scheme in a Microprocessor

In a microprocessor implementation, the switching modes are stored in the memory as a look-up table with the positions of **I**, **E**, and $\Delta\mathbf{I}$ combined as its addresses. The positions of **I** and $\Delta\mathbf{I}$ are coded according to Fig. 6(b), and the position of **E** is coded according to Fig. 6(c). A neutral point voltage control bit (NPVC) is attached to the LSB of this address. When the NPVC is set to "1" by the neutral point voltage feedback control, the switching modes selected will produce a positive neutral current I_n to charge the neutral point voltage up toward the positive dc bus. On the other hand, if NPVC is set to "0," the neutral point voltage will decrease.

Table III shows a portion of the look-up table implemented on a microprocessor. It is translated from Table II. The position of the hexagon in Fig. 6(a) denotes that the current vector **I** stays in the region 1, 0, 0 in Fig. 6(b). From Fig. 6(c), it is determined that the region code of **E** is 0, 1, 0.

IV. SYSTEM IMPLEMENTATION

A prototype of the proposed rectifier has been built using IGBT's as the main power circuit switches and the MO-

TABLE III
SWITCHING MODE SELECTION SCHEME (A LOOK-UP TABLE FOR MICROPROCESSOR IMPLEMENTATION)

Address				Memory
Position of **I**	Position of **E**	Position of Δ**I**	NPVC	Switching modes
.	.	.	.	.
.	.	.	.	.
.	.	.	.	.
100	010	001	0	100
100	010	001	1	0-1-1
100	010	010	*	1-10
100	010	011	0	100
100	010	011	1	0-1-1
100	010	100	*	000
100	010	101	0	100
100	010	101	1	0-1-1
100	010	110	*	0-10
.	.	.	.	.
.	.	.	.	.
.	.	.	.	.

* -- don't care

TOROLA DSP56000 microprocessor as its controller. The control schematic of the prototype rectifier is shown in Fig. 7. In this implementation, a counter with its content synchronized to the electrical angle of ac power supply was used as the reference for the position of the current command and the vector **E**. The resistors $R1$ and $R2$ were used to create the reference for measuring the dc bus neutral point voltage.

It can be determined from Fig. 6(a) that during each transition from one switching mode to another, the number of switches operated ranges from one to three. Therefore, the average switching cost for a transition will be two if equal probability is assumed. Based on this assumption, the average switching frequency for an individual IGBT will be one-third of the sampling frequency since the total number of IGBT's is six in the circuit. In the test system, a sampling frequency of 7 kHz was measured. Therefore, the switching frequency of an IGBT is estimated at about 2.5 kHz.

As the rectifier has the boost type operation characteristic, closed-loop dc bus voltage control is generally required in an actual application. However, as the load of the rectifier can be very well-determined in laboratory test conditions, open-loop control of the dc bus voltage is possible in this case. During the test, the input power was pre-calculated according to the input current command and the fundamental input power factor. After the input power was known, the load resistance was then preset and carefully adjusted during operation to maintain the input and output power balance at a desired dc bus voltage level. For boost type operation, the dc bus voltage must be larger than the peak value of the line-to-line voltage of ac power supply.

The parameters of the system are listed as follows:
ac supply voltage: 115 V, 60 Hz;
dc bus voltage: 300 V;
dc capacitors: 2 × 1000 μF;
Input reactors: 3 × 3.5 mH.

V. EXPERIMENTAL RESULTS

For purpose of comparison, both a hysteresis current controller and the proposed current control scheme were implemented. The waveforms of the three phase input currents i_a, i_b, i_c, and the integration of the neutral current i_n when the hysteresis controller is used are shown in Fig. 8. The reason for showing the integration of the neutral current is that it is proportional to the drift value of neutral point voltage. The same waveforms under the control of the proposed current control scheme are shown in Fig. 9. Although the input current deviations in Fig. 8 are smaller than those in Fig. 9, the

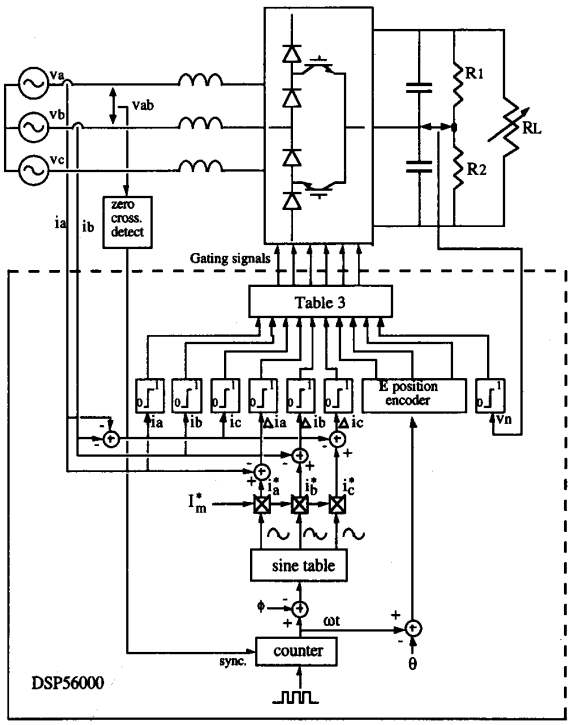

Fig. 7. Control schematic diagram.

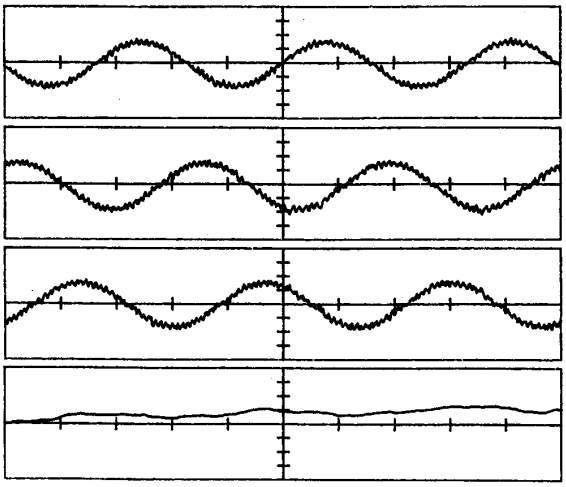

Fig. 8. Experimental results using hysteresis current controller (from top to bottom). Traces 1, 2, 3: phase A, B, C input current, 5 A/div. Trace 4: integration of neutral current I_n.

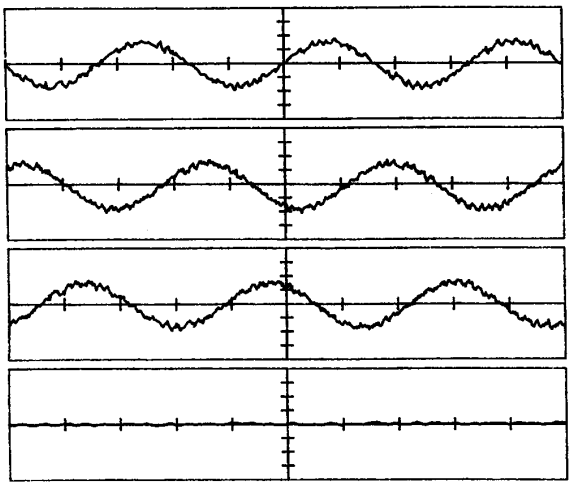

Fig. 9. Experimental results using proposed current regulation scheme (from top to bottom). Traces 1, 2, 3: phase A, B, C input current, 5 A/div. Trace 4: integration of neutral current I_n.

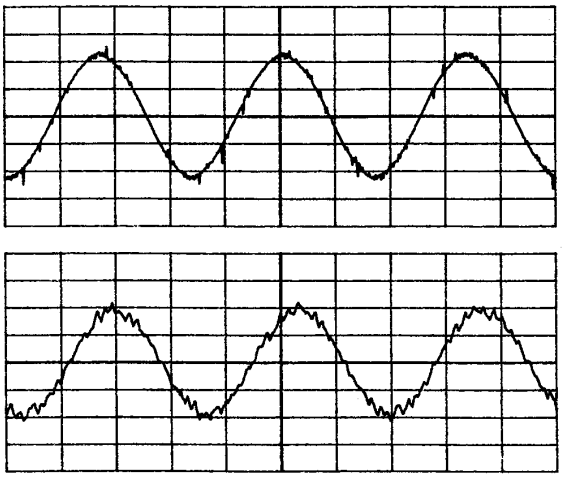

Fig. 10. Experimental result for 30° lagging operation. Trace 1: phase A voltage, 50 V/div. Trace 2: phase A current, 5 A/div.

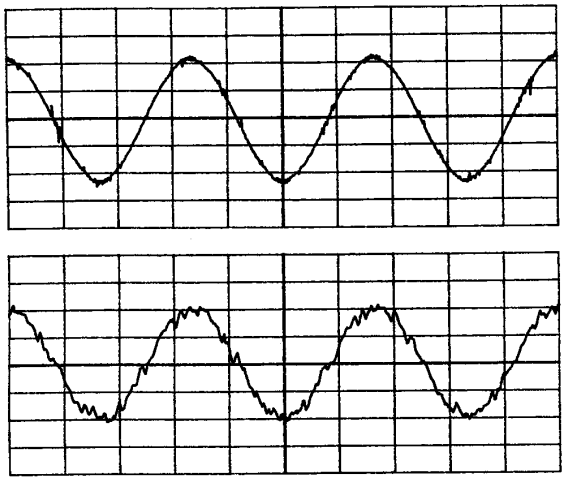

Fig. 11. Experimental result for unity power factor operation. Trace 1: phase A voltage, 50 V/div. Trace 2: phase A current, 5 A/div.

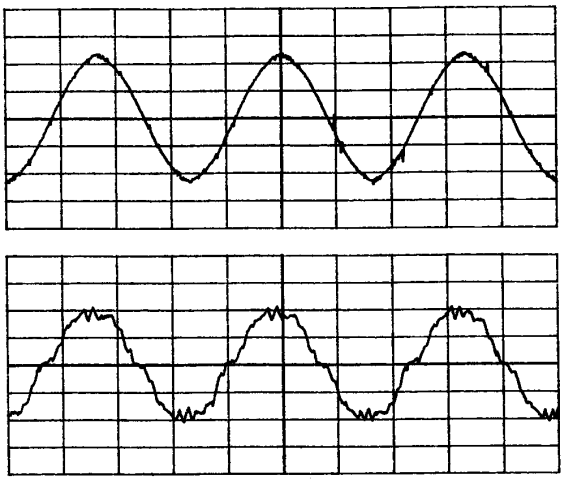

Fig. 12. Experimental result for 30° leading operation. Trace 1: phase A voltage, 50 V/div. Trace 2: phase A current, 5 A/div.

increasing neutral current integration waveform indicates the neutral point voltage drift associated with the hysteresis current control scheme. It should be pointed out that the neutral point voltage was forced balanced by the use of asymmetrical loads connected to the two dc bus capacitors separately when the hysteresis controller was used, otherwise the neutral point voltage would continually drift. As a result, hysteresis control was not able to function properly. On the other hand, when the proposed control scheme was used, as can be seen from Fig. 9, although the current deviation is slightly larger due to the compromise between the input current and the neutral point voltage control, the neutral point voltage was balanced successfully and thus satisfactory operation can be guaranteed.

The ac power supply phase voltage and input current shown in Fig. 10–12 demonstrate the feasibility of power factor adjustment. The rectifier was operated with fundamental power factors of 30° lagging in Fig. 10, unity power factor in Fig. 11, and 30° leading in Fig. 12 respectively. Low frequency current distortions can be found during 30° leading operation as predicted in the steady state analysis.

VI. Conclusion

A new type of utility interface, a force commutated three level boost type rectifier is proposed in this paper. The interface draws nearly sinusoidal currents from the three phase utility with a power factor near unity and offers inherent characteristics of absence from shoot-through current as well as balanced voltage stress on devices (1/2 the dc bus voltage). Therefore this new rectifier has the features of high reliability, simple control, and high output of dc bus voltage. A combined input current and neutral point voltage control scheme is also being developed.

ACKNOWLEDGMENT

The authors wish to thank Ben Banerjee and the Electric Power Research Institute for support of this work.

REFERENCES

[1] A. Nabae, I. Takahashi, and H. Akagi, "A new neutral-point- clamped PWM inverter," *IEEE Trans. Ind. Applicat.*, vol. 17, no. 5, pp. 518–523, Sept./Oct. 1981.

[2] A. Nabae, S. Ogasawara, and H. Akagi, "A novel control scheme for current-controlled PWM inverters," *IEEE Trans. Ind. Applicat.*, vol. 22, no. 4, pp. 697–701, July/Aug. 1981.

[3] S. Ogasawara and H. Akagi, "A vector control system using neutral-point-clamped voltage source PWM inverters," *Conf. Rec. of IEEE Ind. Applicat. Soc. Ann. Meeting*, Dearborn, MI, Sept. 28-Oct. 4, 1991, vol. 1, pp. 442–427.

[4] Y. Tadros, S. Salama, and R. Höf, "Three level IGBT inverter," *23rd Ann. Power Electron. Specialists Conf.*, Toledo, Spain, 1992, pp. 46–52.

[5] T. Takeshita and N. Matsui, "PWM control and input characteristics of three-phase multi-level AC/DC converter," *23rd Ann. Power Electron. Specialists Conf.*, Toledo, Spain, 1992, pp. 175–180.

Yifan Zhao, for a photograph and biography, please see page 106 of this issue.

Yue Li received the B.Sc. degree from Tsinghua University, Beijing, China, in 1983, and the M.S. degree from the First Academy of the Astronautics Ministry of China, Beijing, in 1986.

Since 1991, he has been with the Department of Electrical and Computer Engineering at the University of Wisconsin, Madison, WI, where he is currently a Ph.D. candidate, engaged in the area of electric machine design and drives. He has also participated as a researcher for several industrial projects.

Thomas A. Lipo (M'64–SM'71–F'87), for a photograph and biography, please see page 106 of this issue.